Optical rotation by plasmonic circular dichroism of isolated gold nanorod aggregates

Kamalesh Chaudhari and Thalappil Pradeep

Citation: Applied Physics Letters **105**, 203105 (2014); doi: 10.1063/1.4902318
View online: http://dx.doi.org/10.1063/1.4902318
View Table of Contents: http://scitation.aip.org/content/aip/journal/apl/105/20?ver=pdfcov
Published by the AIP Publishing

Optical rotation by plasmonic circular dichroism of isolated gold nanorod aggregates

Kamalesh Chaudhari[1,2] and Thalappil Pradeep[2,a)]
[1]*Department of Biotechnology, Indian Institute of Technology Madras, Chennai 600 036, India*
[2]*DST Unit of Nanoscience (DST UNS) and Thematic Unit of Excellence (TUE), Department of Chemistry, Indian Institute of Technology Madras, Chennai 600 036, India*

(Received 17 October 2014; accepted 8 November 2014; published online 19 November 2014)

We show that plasmonic chirality in single gold nanorod (GNR) aggregates leads to the rotation of polarization of the scattered light. 3D glasses in conjunction with linearly polarized dark field scattering microspectroscopy were used to study the chirality of single GNR aggregates. Using this hetero-polarizer setup, we not only detect but also quantify their chirality. A polar mapping strategy was used for providing direct evidence for the emergence of light of different polarization angles when chiral GNR aggregates were excited with circularly polarized light of different handedness. Further, we have developed a methodology to eliminate fluctuations in the scattering intensity by averaging and normalizing the data. This allows calculation of plasmonic circular dichroism scattering spectra with high accuracy. © *2014 AIP Publishing LLC*.
[http://dx.doi.org/10.1063/1.4902318]

Diverse combinations of chiral molecules and arrangements of nanoparticles exhibit plasmonic circular dichroism (PCD).[1–6] The origin of PCD may be different in each of these combinations. Chiral molecules which otherwise exhibit circular dichroism (CD) signals in the UV range, if inserted within the plasmonic hot spots, exhibit giant enhancement in the same.[7] This enhancement arises from the coulomb interaction of the molecular dipoles parallel to the axis of the dimers of nanoparticles.[7] But for nanocrystals such as Au-twisters or pyramid-like and tetrahedral crystals of gold, chirality is intrinsic and CD is induced by mixing of different plasmon harmonics.[8] In some cases, when nanoclusters of gold or silver, composed of a few atoms, are stabilized with chiral ligands, the resultant protected clusters exhibit chiroptical properties[5,9] due to the transfer of ligand chirality to the metal core either in its structure or in its electronic states as a result of the perturbation of the electronic field of the ligands.[5] It has been shown that a variety of plasmonic nanoparticle (PNP) assemblies formed on helical molecular templates exhibit plasmonic chirality.[3,4,6,10,11] Interestingly, assemblies of gold nanorods (GNRs) as well as dimers of GNRs also exhibit PCD.[1,12] Auguié *et al.* have shown by theoretical calculations that when inter-particle distance is comparable to the wavelength of incident light, the phase of electromagnetic field coupling two dipoles becomes distance dependent. This leads to retardation effect and gives rise to asymmetric CD line shape.[1] Ma *et al.* have shown the possibility of PCD measurements of such single particles using correlated transmission electron microscopy (TEM) and scattering spectroscopy.[12] Although such advanced measurements are necessary for testing the validity of concepts; simplification of methods is required for their routine use. For such simplification, new techniques for signal detection as well as understanding of novel phenomena associated with the system under investigation are equally important.

In this work, we show that there is optical rotation involved in the PCD of GNR aggregates and it can be detected using recently developed hetero-polarizer setup. These aggregates were formed as a result of interaction between GNRs of size ~30/10 nm (length/diameter) and L-glutathione, a tripeptide (GSH). Details of the method of preparation are provided in the supplementary material.[13] TEM images of few such GNR aggregates are shown in

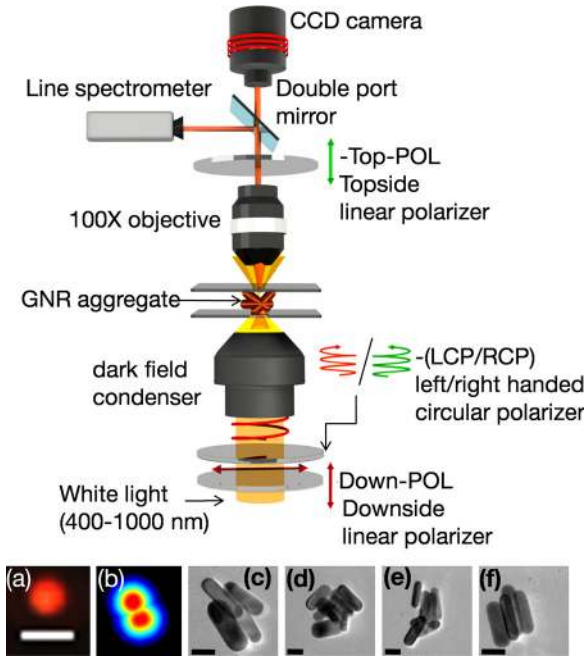

FIG. 1. A hetero-polarizer setup to sense and quantify PCD signals at single particle level, consisting of 3D glasses and linear polarizers on an upright DFSMS setup. First two images ((a) and (b)) at the bottom left show a single GNR as seen in DFSMS along with its polar map, respectively. Scale bar is 1 μm. Next four images ((c)–(f)) are TEM images of single isolated GNR aggregates. Scale bar is 20 nm. GNRs aligned with off-axis tilt, even minor, are likely to be chiral.[1,12] The symbols and codes for polarizers will be used in the next figures.

a)E-mail: pradeep@iitm.ac.in

Fig. 1 (see below). Few more images are shown in the supplementary material.[13] In dark field scattering microspectroscopy (DFSMS) studies, GNR aggregation was confirmed by changes in their scattering spectrum while analyzing the PCD data. From the previous studies, it has been observed that single particle spectra of end-to-end or side-by-side arrangements of GNRs give rise to a single prominent plasmonic band (in contrast to two peaks in the ensemble spectra in solution) but other arrangements give rise to two plasmonic bands.[14,15] Hence, existence of two plasmonic bands confirms the presence of GNR aggregates.

To sense and quantify PCD signals at single particle level, a simple hetero-polarizer based technique was developed. This technique utilizes regular 3D glasses as circular polarizers for illumination of the samples in linearly polarized-DFSMS (PDFSMS). Details of the experimental setup are shown in Fig. 1. Please note that although 3D glasses themselves are analyzers of circularly polarized light (CPL) (quarter wave plate + linear polarizer), to provide uniform linearly polarized input to the quarter wave plate, LCP/RCP (left/right handed circular polarizers) were placed after Down-POL (downside polarizer, Fig. 1) in the imaging setup. Recent studies from our group have shown that when scattering from isolated GNRs was analyzed with a linear analyzer having a minute tilt, their polarization patterns can be mapped (referred as polar maps, Fig. 1 inset).[16] Such maps are formed due to refraction of light rays when they pass through an analyzer. This technique provides *in situ* mapping of the polarization patterns of nanostructures which selectively scatter light of specific polarization. Isolated rod shaped particles exhibit "figure 8" shaped polar map, while isotropic spherical particle exhibits a filled circle. For this purpose, scattered light from the sample was passed from linear analyzer (Top-POL, topside polarizer) whenever polar mapping was required. Since polar maps, being projections of maximum intensity values from a set of images captured at various analyzer angles, they span a larger area than the actual GNR image. Hence, size of the polar map depends on the extent of shift in GNR image which occurs due to refraction of scattered light through analyzer with minute angular tilt.[16] Decrease in the scattering intensity due to polarizers in the optical path was taken care of by increasing the exposure time of the camera. Note that the diffraction limited images of single GNRs are spherical in shape and are red in color due to the excitation of longitudinal plasmon.

Previous reports using ensemble CD spectroscopy have shown that when GNRs are treated with GSH, they exhibit chiral response.[17] Chirality of GNR aggregates can be attributed to the arrangements in which longitudinal axis of GNRs are crossed[1,12] as in TEM images (Figs. 1(c)–1(f)). In the case of single particle spectroscopic measurements, different arrangements of aggregates can settle on the glass substrate with different orientations. Hence, when such aggregates having different orientations were studied, some of them exhibit strong chirality whereas others do not. Also due to randomness in the orientation and arrangements of GNR aggregates, there can be variations in the PCD signals. Due to the same reason, results from single particle spectroscopic measurements cannot be compared with ensemble measurements. Such measurements performed on a chiral and non-chiral GNR aggregate (referred as CGNR and NCGNR, respectively) are discussed below.

Scattering spectra of CGNR and NCGNR confirm that these are indeed aggregates and not single GNRs (Fig. 2(a)).[14,15] Figure 2(b) shows the polar plots of CGNR and NCGNR. Polar plots are calculated by integrating the grayscale intensity over

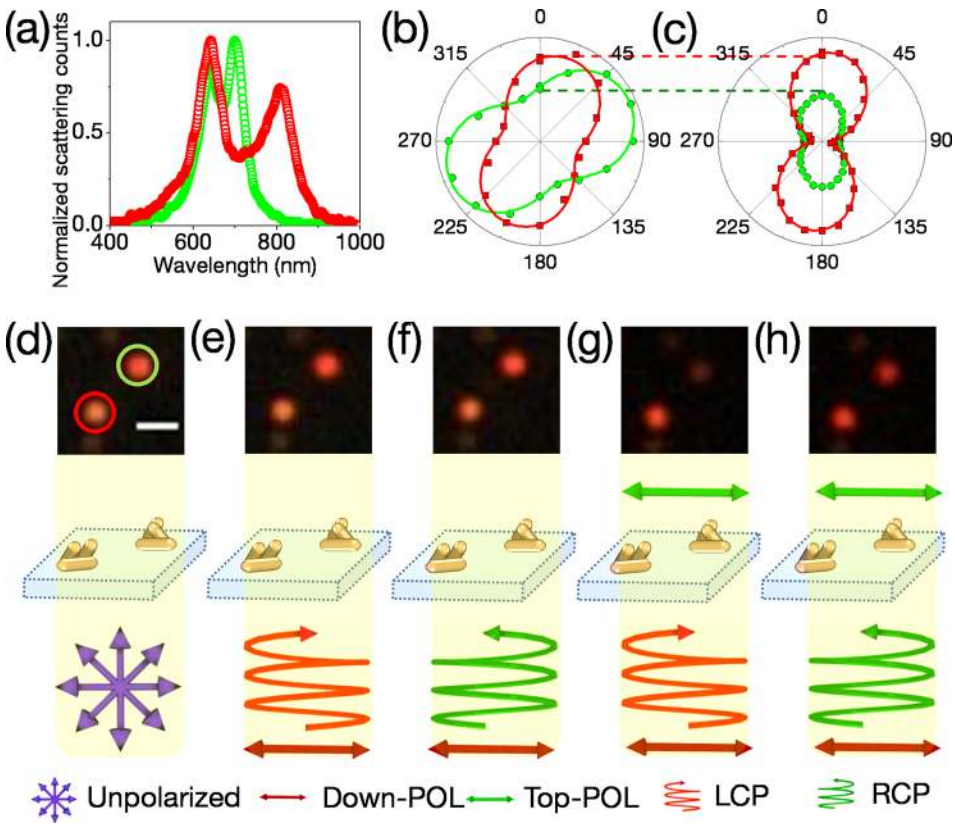

FIG. 2. (a) Scattering spectra of GNR aggregates. Colors correspond to the encircled GNR aggregates shown in the image (d). Chiral GNR aggregate is encircled with green color and non-chiral GNR aggregate is encircled in red color. (b) Polar plots for two gold nanorod aggregates are shown in corresponding color. (c) Polar profile of GNR aggregates when orientation of Top-POL was kept constant and Down-POL was rotated. (d)–(h) Scale bar is 1 μm. Combinations of polarizers for each measurement ((d)–(h)) are shown below the images. Further details are provided in Fig. 1. (Multimedia view) [URL: http://dx.doi.org/10.1063/1.4902318.1]

the image spot of the particle as reported previously.[16] Fig. 2(c) shows that when both Top-POL and Down-POL are parallel (0°/180°), relative scattering intensity of CGNR and NCGNR can be correlated with the one observed when only Down-POL was used (Fig. 2(b)). At other angles, changes in the scattering intensity follow the same trend, which are due to changes in the transmittance when Down-POL is rotated with respect to Top-POL. These data are used to quantify chirality of particles as described in the subsequent discussion. Images of CGNR and NCGNR nanoaggregates captured with unpolarized white light illumination are shown in Fig. 2(d). For unpolarized illumination, both these aggregates exhibit intense scattering signals in DFSMS images. When circular polarizers (LCP/RCP) were placed after Down-POL, both the aggregates exhibit intense scattering spots similar to the case of unpolarized illumination (Figs. 2(e) and 2(f)). This is because CPL also allows excitation of plasmon resonances along all the axes. Then to check whether polarization of scattered light has any dependence on the handedness of illumination, PDFSMS measurements were performed. In these measurements, samples were illuminated with circularly polarized light generated by LCP/RCP and subsequent scattering signal was detected through Top-POL. By comparing Figs. 2(g) and 2(h), we see that CGNR exhibits substantial change in the scattering intensity whereas NCGNR remains almost constant. This was attributed to the strong chirality of CGNR. Please also note that this can be observed only when Top-POL is in the optical path (compare Figs. 2(e) and 2(f), where the experiment is the same as Figs. 2(g) and 2(h), except that Top-POL is not in the optical path). Repeatability of these measurements is shown in Fig. 3(a). See multimedia view of Fig. 2(g) showing images of CGNR and NCGNR captured upon alternate RCP and LCP illumination along with few more chiral and non-chiral GNR aggregates. It implies that this behavior is indeed due to chirality of nanoaggregates and not due to rotation of loosely bound aggregates or other random fluctuations. From this data, we see that CGNR consistently goes through substantial change (% change) in the scattering intensity when illuminated alternatively with RCP and LCP light. But NCGNR scattering intensity remains almost constant upon illumination with LCP/RCP.

From Fig. 3(a), we see that scattering intensity of CGNR drops to ~50% when illumination changes from RCP to LCP. These results suggest that one can illuminate sample with LCP/RCP and follow the changes in the linear polarization of the scattered light (Φ) by monitoring the transmitted light intensity through Top-POL. This difference in transmission is interpolated to obtain angular change in polarization of scattered light (Fig. 3(b)). Note that Fig. 3(b) is an alternate representation of Fig. 2(c). The curves in Fig. 3(b) may be fitted with the following equation:

$$\%I = C + a\cos^4(\theta - \beta), \tag{1}$$

where, θ is the angular position of Down-POL with respect to Top-POL, C is the constant baseline, a is a multiplier which helps in matching the amplitude of $\cos^4(\theta)$ with actual signal, and β indicates shift in θ. Fig. 3(b) marks the parameter Φ for CGNR, for which it comes out as ~60° where scattering intensity changes from 100% to 50%. This parameter is a good measure of the PCD of GNR aggregates and takes

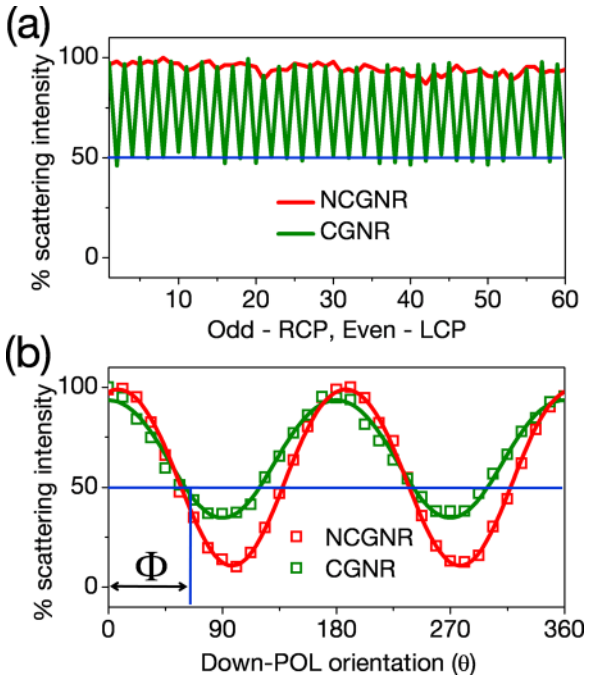

FIG. 3. (a) Percentage changes in the variation of the scattering intensity for CGNR and NCGNR plotted against the handedness of circularly polarized illumination. Odd numbers on X scale presents RCP illumination and even numbers present LCP illumination. (b) Polar profile of CGNR and NCGNR when Top-POL was kept constant and Down-POL was rotated.

values from 0–90 in units of degrees. Thus, chirality may be quantitated as

$$\Phi = \left| \cos^{-4}\left(\frac{\%I_{LCP<90} - C}{a}\right) - \cos^{-4}\left(\frac{\%I_{RCP<90} - C}{a}\right) \right|, \tag{2}$$

where, $\%I_{LCP<90}$ and $\%I_{RCP<90}$ are scattering intensities collected through Top-POL upon illuminating the sample with LCP and RCP light, respectively. Percentage values of $I_{LCP<90}$ and $I_{RCP<90}$ used in this formula are for θ values less than 90°, each percentage maximum is determined amongst $I_{LCP<90}$ and $I_{RCP<90}$. Maximum change in linear polarization occurs between 0° and 90°.

To provide direct evidence of optical rotation, we use the polar mapping technique reported before.[16] Figures 4(a)–4(c) show the results of mapping done over two GNR aggregates with unpolarized, LCP and RCP illumination, respectively. Corresponding PCD spectra are shown in Fig. 4(d). For aggregate "1," polar map is symmetric throughout the observation, but for aggregate "2" it exhibits complex asymmetric polar maps when illuminated with light of different polarizations. This can be attributed to excitation of multiple plasmon axes. Polar map of aggregate "2" with LCP illumination shows selection of specific polarization in scattered light (Fig. 4(b)) and this subsequently changes when illumination was changed to RCP. Polar plots determined by integration of the scattering intensity over the image area of individual GNR aggregates are given in the supplementary material[13] to further support the mapping data.

The results discussed above show that quantification of chirality can be done by PDFSMS. Although such quantification is possible by detecting optical rotation through Top-

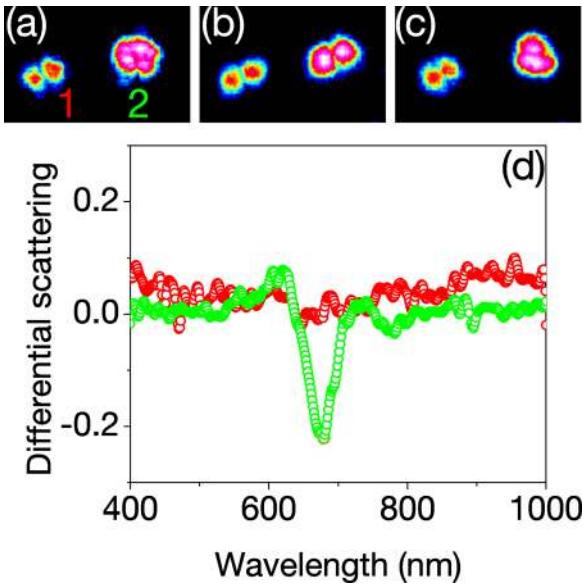

FIG. 4. Polar maps of CGNR (green) and NCGNR (red) aggregates upon three different dark field illuminations: (a) Unpolarized, (b) LCP, and (c) RCP. Two aggregates are designated as "1" and "2" in (a). For nonchiral aggregate "1" map remains almost same whereas for chiral aggregate "2" map changes drastically when the type of illumination is changed. (d) Corresponding PCDS spectra are shown for GNR aggregates, "1" and "2" in corresponding colors.

POL, there can be minute differences between images when same chiral GNR aggregate is observed at RCP/LCP illumination without Top-POL (Figs. 2(e) and 2(f)). Hence, for the determination of single particle PCD scattering (PCDS) spectra, more sensitive measurements or noise removal technique is required. Supplementary material[13] describes this methodology. Briefly, it is based on simple normalization of the spectroscopic data which helps in the reduction of quantitative variations in the scattering intensity but conserves the qualitative changes due to chirality. Normalization leads to noise removal as PCDS involves wavelength dependent changes in the scattering intensity and not an overall increase in scattering intensity. PCDS spectra determined using such calculations are shown in Fig. 4(d).

In summary, we have shown that there is optical rotation involved in the plasmonic circular dichroism of single GNR aggregates. This was detected efficiently using a heteropolarizer-based setup. It is as simple composed of a combination of regular DFSMS along with 3D glasses. Observations have shown that the differential scattering property was greatly amplified when the detection was done through a linear analyzer. The major benefits of this methodology are that it is simple, easy to perform, and quick measurements can be done over a large area of the sample. Cases in which ensemble spectroscopy cannot resolve the complexity of various components contributing the CD spectra, this kind of single particle measurements will be useful. We believe that the phenomena of chirality dependent optical rotation will be of prime importance in the development of new sensing and characterization techniques in materials science and biology.

We thank the Department of Science and Technology, India for constantly supporting our research on nanomaterials.

[1]B. Auguié, J. L. Alonso-Gomez, A. Guerrero-Martinez, and L. M. Liz-Marzan, J. Phys. Chem. Lett. **2**, 846 (2011).
[2]W. Ma, H. Kuang, L. Xu, L. Ding, C. Xu, L. Wang, and N. A. Kotov, Nat. Commun. **4**, 2689 (2013).
[3]Y. Tsuchiya, T. Noguchi, D. Yoshihara, T. Yamamoto, T. Shiraki, S. I. Tamaru, and S. Shinkai, Supramol. Chem. **25**, 748 (2013).
[4]Z. Fan and A. O. Govorov, J. Phys. Chem. C **115**, 13254 (2011).
[5]M. Farrag, M. Tschurl, and U. Heiz, Chem. Mater. **25**, 862 (2013).
[6]A. Kuzyk, R. Schreiber, Z. Fan, G. Pardatscher, E.-M. Roller, A. Hoegele, F. C. Simmel, A. O. Govorov, and T. Liedl, Nature **483**, 311 (2012).
[7]H. Zhang and A. O. Govorov, Phys. Rev. B **87**, 075410 (2013).
[8]Z. Fan and A. O. Govorov, Nano Lett. **12**, 3283 (2012).
[9]O. Lopez-Acevedo, H. Tsunoyama, T. Tsukuda, H. Hakkinen, and C. M. Aikens, J. Am. Chem. Soc. **132**, 8210 (2010).
[10]W. Liu, D. Liu, Z. Zhu, B. Han, Y. Gao, and Z. Tang, Nanoscale **6**, 4498 (2014).
[11]G. Shemer, O. Krichevski, G. Markovich, T. Molotsky, I. Lubovitz, and A. B. Kotlyar, J. Am. Chem. Soc. **128**, 11006 (2006).
[12]W. Ma, H. Kuang, L. Wang, L. Xu, W.-S. Chang, H. Zhang, M. Sun, Y. Zhu, Y. Zhao, L. Liu, C. Xu, S. Link, and N. A. Kotov, Sci. Rep. **3**, 1934 (2013).
[13]See supplementary material at http://dx.doi.org/10.1063/1.4902318 for methods, supporting data and video.
[14]A. M. Funston, C. Novo, T. J. Davis, and P. Mulvaney, Nano Lett. **9**, 1651 (2009).
[15]L. Shao, K. C. Woo, H. Chen, Z. Jin, J. Wang, and H.-Q. Lin, ACS Nano **4**, 3053 (2010).
[16]K. Chaudhari and T. Pradeep, Sci. Rep. **4**, 5948 (2014).
[17]Z. Zhu, J. Guo, W. Liu, Z. Li, B. Han, W. Zhang, and Z. Tang, Angew. Chem. Int. Ed. **52**, 13571 (2013).